

Observation of Combined Josephson and Charging Effects in Small Tunnel Junction Circuits

T. A. Fulton, P. L. Gammel, D. J. Bishop, and L. N. Dunkleberger
AT&T Bell Laboratories, Murray Hill, New Jersey 07974

G. J. Dolan

Department of Physics, University of Pennsylvania, Philadelphia, Pennsylvania 19104
(Received 3 May 1989)

Experiments on small superconducting tunnel junctions in a Giaever-Zeller-plus-SQUID geometry clearly show an $I(V)$ feature due to Josephson supercurrent in a regime where single-electron charging effects are dominant. The $I(V)$ data exhibit marked oscillations with gate voltage characteristic of single-electron charging. The Josephson feature shows both this effect and SQUID-related oscillations with applied magnetic field. The behavior can be understood through the usual model for charging effects in such circuits, extended to include two-electron transitions.

PACS numbers: 74.50.+r

In small superconducting tunnel junctions charging and Josephson effects compete in that they involve non-commuting operators for the charge imbalance and the Josephson phase difference. The relevant parameters are the single-electron charging energy $E_c = e^2/2C$, where C is the effective capacitance and the Josephson coupling energy $E_J = \hbar I_c/2e$, where I_c is the maximum tunnel supercurrent. For $E_c/E_J \gg 1$ one expects well-defined charging effects and suppressed Josephson effects, and vice versa for $E_c/E_J \ll 1$. Experiments on charging effects typically employ low- C junctions of dimensions $\sim 0.1 \mu\text{m}$. Resistances R are often large as well which reduces E_J according to $I_c = \pi 2\Delta/4R$, where 2Δ is the superconducting energy gap. Several such experiments, having $E_c/E_J \gg 1$, have used Giaever-Zeller (GZ) circuits,¹⁻⁶ which in essence have two junctions in series with a low-capacitance central region. These showed clear charging effects in the current-voltage characteristics $I(V)$ due to the single-(quasi)particle tunneling current I_q , but coexisting Josephson-related behavior was not reported. Other workers have examined single- and multiple-junction circuits^{7,8} estimated to be in the region around $E_c/E_J \sim 1$. These showed unusual Josephson behavior around $V=0$, much of which was interpreted as due to the interplay of Josephson and charging effects, as was earlier work with point-contact SQUID's.⁹ Theoretical interest in this regime, $E_c \gtrsim E_J$, has focused on Bloch oscillations in single junctions¹⁰⁻¹⁴ and the interaction of charging effects with I_q .^{10,15,16}

We report experiments that show a clear case of coexisting Josephson and charging effects, for $E_c/E_J \sim 5$. Both effects appear prominently in the $I(V)$ curves of tunnel junctions in a GZ geometry. The circuits are like those of Ref. 2 with the important addition that one junction is replaced with a two-junction SQUID. This allows identification of the $I(V)$ features arising from Josephson currents in the SQUID with the familiar oscillatory dependence on magnetic field B . The observations can be understood by extending the semiclassical model

of charging effects in GZ circuits, involving I_q -induced one-electron transitions between discrete charge states, to include Josephson-induced two-electron transitions. While the effects are related to single-junction Bloch oscillations, they involve a distinct, unanticipated process that depends on the multijunction nature of the circuit.

In a GZ circuit the central electrode has discrete electrostatic voltage and energy levels dependent on the charge state. The levels can be shifted by a voltage V_M applied to an adjacent gate electrode, so the shape of the $I(V)$ is modulated (periodically) by V_M .^{2,17} This modulation is our main experimental tool for study of charging effects and often provides a direct measure of circuit capacitances and E_c .

The two configurations used are sketched in Figs. 1 and 2. Three or four roughly square Al tunnel junctions ($2\Delta \sim 0.4 \text{ mV}$), of dimensions $\lesssim 0.1 \mu\text{m}$, make contact to a central bar of dimensions $\sim 1 \times (0.1-0.5) \mu\text{m}^2$. Fabri-

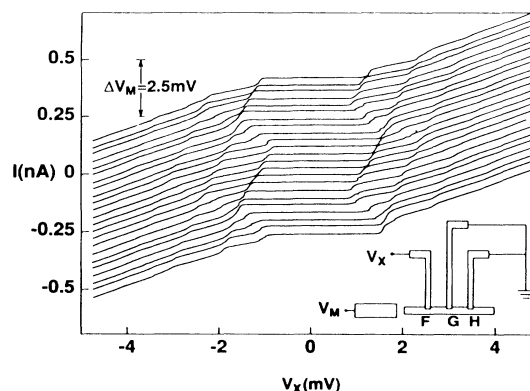


FIG. 1. $I(V_x)$ for a series of V_M for the circuit at lower right. The gate electrode, shown schematically at the left of the circuit, is actually formed by the underlying substrate as described in Ref. 2.

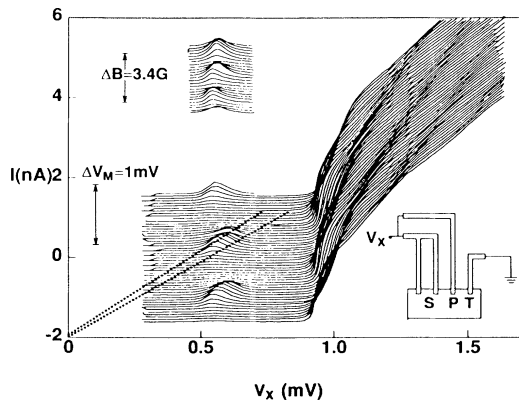


FIG. 2. Lower curves: A portion of the $I(V_X)$ for a series of V_M for the circuit at lower right. Dotted lines as described in text. Upper curves: The B dependence of the peak.

cation was as in Ref. 2. The multijunction nature allows measurement of R for each junction. As the $I(V)$ curves are most readily interpreted for the two junctions in series, connections are made as in, e.g., Fig. 1 where F is connected to the voltage bias (V_X) and G and H to ground. Then G and H see the same bias and act as one junction. Note that in Fig. 2 the left-most junction leads are connected a few microns away to form the superconducting interferometer, or SQUID.

The sample sketched in Fig. 1 had junction dimensions $\sim 0.05 \mu\text{m}$. This sample, which showed no Josephson behavior, provides our best example of the interaction of charging effects and I_q , and of the validity of the semiclassical model in this regime. The junction resistances were $\sim 7\text{--}8 \text{ M}\Omega$ and the measured capacitance C' , defined below, was $\sim 0.2 \text{ fF}$, giving $E_c/E_J = 6 \times 10^3$. Figure 1 shows a set of $I(V_X)$, at $T \sim 0.2 \text{ K}$, spaced by their fixed values of V_M . Each has high resistance at low V_X , an onset of I at various $V_X \sim 1 \text{ mV}$, and several steps in I at higher V_X . The shape of $I(V_X)$ varies markedly and periodically with V_M , and the positions in V_X vs V_M of the onset and steps in I form patterns of intersecting straight lines.

To review the model^{1,15-17} (see the circuit in Fig. 3), subscripts X, Y, Z , and M refer to the bias, central, ground, and modulation electrodes. There are voltages $V_X, V_Y, V_Z = 0$, and V_M , junctions J_{XY} and J_{YZ} , capacitances C_{XY}, C_{YZ} , and C_{YM} whose sum is C' , and N , the excess number of electrons on Y . (For simplicity we pretend electrons are positive.) Current I flows from X to Z by stochastic tunneling of electrons through J_{XY} and J_{YZ} at rates dependent on $V_X - V_Y$ and V_Y . The central voltage obeys $V_Y = (C_{XY}/C')V_X + (C_{YM}/C')V_M + Ne/C'$ ($N = 0, \pm 1, \dots$). These discrete V_Y levels, spaced by e/C' , shift with V_X and V_M . As changing V_M by e/C_{YM} shifts the levels by e/C' , the shape of $I(V_X)$ oscillates with V_M

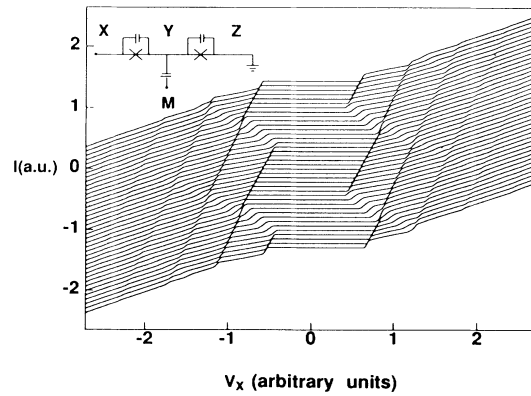


FIG. 3. Simulated $I(V_X, V_M)$ for the circuit at upper left.

with this period. The rate P_{YZ} , say, at which electrons tunnel from Y to Z through J_{YZ} at initial bias V_Y , resembles in shape a superconducting tunnel junction $I(V)$ displaced to higher bias by $e/2C'$ [see Fig. 4(a)], being small for $V_Y < 2\Delta + e/2C'$ (the energy-gap feature) and large above, and similarly for P_{XY}, P_{YX} ,

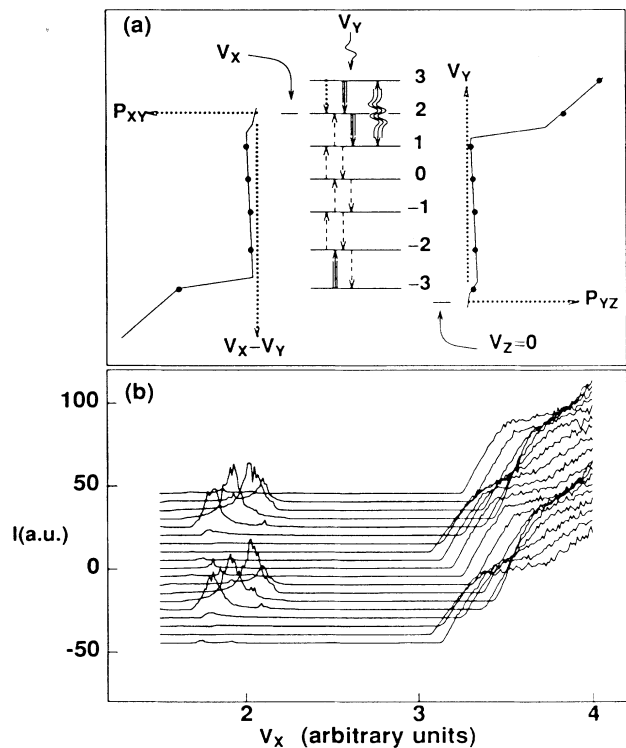


FIG. 4. (a) A charging voltage-level diagram including a two-electron transition. (b) Simulated $I(V_X, V_M)$ based on the model.

and P_{ZY} . With time, the system hops randomly from level N to $N \pm 1$ at rates given by the four P_{ij} . From this model one may simulate $I(V_X, V_M)$, as in Fig. 3. These closely resemble the data of Fig. 1. The increases in I occur on lines of V_X and V_M where V_Y or $V_X - V_Y$ levels pass through the gap feature in the corresponding P_{ij} . Thus lines of $dV_X/dV_M > 0$ come from J_{XY} and have slope $C_{YM}/(C_{YZ} + C_{YM})$, etc. These linear features in Fig. 1 give directly $C_{XY} = 64 \pm 4$ aF, $C_{YZ} = 104 \pm 7$ aF, and $C_{YM} = 41.6 \pm 0.5$ aF. The simulations of Fig. 3 use these values, the measured $R_F = 7.5 \pm 0.25$ M Ω , $R_G = 32.5 \pm 0.5$ M Ω , and $R_H = 8.5 \pm 0.25$ M Ω and a BCS-model P_{ij} with a somewhat broadened gap. Similar agreement of $I(V_X, V_M)$ with simulations is also found for these junctions in the normal state.

Several samples, having $0.5 \lesssim E_c/E_J \lesssim 10$, showed both charging and Josephson behavior. Charging (Josephson) behavior was strong at the higher (lower) end of this range and weak at the other. We focus on one sample of $E_c/E_J \sim 5$, since understanding Josephson behavior in the presence of strong charging effects seems of special interest (and a prerequisite for study of the intermediate range). Also we can hope to understand the behavior as a perturbation on the charging model. The sample is a SQUID plus two single junctions (of dimensions ~ 0.1 μm) in contact with a central region, connected as in Fig. 2. The measured R 's were 98.2 ± 2 , 169 ± 2 , and 163 ± 2 k Ω for the SQUID S and junctions P and T , respectively. The measured C' was 1.5 fF (reflecting the larger sizes), giving $E_c \sim 8 \times 10^{-24}$ J, while the nominal E_J for $S + P$ ($R \sim 62$ k Ω) is $\sim 1.5 \times 10^{-24}$ J. The lower curves in Fig. 2 are a set of the $I(V_X, V_M)$ in the region $0.3 < V_X < 1.5$ mV, at $T \sim 0.35$ K. Above the gap the shapes resemble those in Fig. 1, although the charging-effect structure is weaker due to the smaller e/C' . From the structure one obtains $C_{XY} = 970 \pm 90$ aF, $C_{YZ} = 324 \pm 50$ aF, and $C_{YM} = 193 \pm 3$ aF.

The Josephson-related feature is the current peak of ~ 0.3 nA at ~ 0.55 mV. It shows strong periodic modulation in amplitude and some in position with V_M . Confirmation that this peak involves Josephson effects come from the B dependence shown in the upper curves in Fig. 3. These are a series of $I(V_X)$ curves taken around the peak spaced by the corresponding increments in B . The V_M was fixed at a value for which the peak was large. The peak amplitude oscillates with B with a 1.7 G period. The same period is seen in this geometry for low- R samples dominated by Josephson effects, and is reasonable for the ~ 8 - μm^2 loop area, allowing for field enhancement by flux diversion from nearby superconducting areas. The peak and its companion at $V_X < 0$ oscillate in phase and are largest at $B = 0$. Part of the peak may be due to junction P . For the region $V_X < 0.4$ mV, not shown in Fig. 2, I remains small with weak B and V_M -dependent thermally activated structure invisible on the scale of Fig. 2 at this temperature. No struc-

ture near $V_X = 0$ of the sort described, e.g., in Ref. 8 is seen.

This behavior can be accounted for by including two-electron transitions in the charging model, as in Fig. 4(a). Shown are the bias V_X , $V_Z = 0$, and the V_Y levels labeled by N , along with the rates P_{XY} and P_{YZ} drawn so that the V_Y levels intersect at the proper bias points. (We neglect P_{YX} and P_{ZY} .) The spacings correspond roughly to the sample of Fig. 2 biased at the current peak. Previously we considered just the $N \rightarrow N \pm 1$ I_q transitions, indicated by straight arrows whose weights reflect the rates. To review, suppose that $-2 \leq N \leq 1$. As P_{XY} and P_{YZ} are small, the system jumps slowly, randomly between neighboring levels. If it reaches $N = 2$ then because P_{YZ} is large (above the gap) an electron soon tunnels from Y to Z , causing a quick return to the $N = 1$ level. Similarly a jump to $N = -3$ soon falls back to $N = -2$.

Now consider the suggested additional $N \rightarrow N \pm 2$ Josephson transitions [wavy line in Fig. 4(a)]. These occur because the tunneling Hamiltonian has an effective matrix element of size $E_J/2$ coupling states differing by one electron pair.¹⁸ Suppose for simplicity that $E_J \ll E_c$. Then these states are coupled strongly only when they are nearly equal in energy (in the sense given below). For this circuit this equality occurs whenever any level N happens to lie at $V_Y = 0$ or $V_X - V_Y = 0$. (This occurs periodically with V_M for any fixed V_X .) The two levels involved are $N + 1$ and $N - 1$ (not N). For instance, in Fig. 4(a) the $N = 2$ level is at $V_X - V_Y = 0$. Starting in level 1, no network is required to transfer a pair of electrons from X to Y , ending in level 3. Thus the $N = 1$ and $N = 3$ levels have equal energy in this sense and are separated by two electrons, so they are strongly mixed by the Josephson coupling. In quantum terms, symmetric and antisymmetric combinations of states $|1\rangle$ and $|3\rangle$ are eigenstates and the energies are split by E_J . This mixing of equal-energy N levels is much like that in Bloch oscillation theories.¹⁰⁻¹⁴

We suggest that this mixing causes the current peak through the following multistep process: Suppose that initially $N = 0$ and a $0 \rightarrow 1$ I_q transition occurs to state $|1\rangle$. The Josephson coupling causes an admixture of state $|3\rangle$ to occur, starting perhaps as a coherent oscillation at a rate $\sim E_J/\hbar = I_c/2e$. By itself this $1 \rightleftharpoons 3$ process gives no net dc current. For the bias condition in Fig. 4(a), however, the $N = 3$ level lies well above the gap in P_{YZ} and a $3 \rightarrow 2$ I_q transition, due to an electron tunneling in J_{YZ} , soon interrupts the $1 \rightleftharpoons 3$ mixing. If, as shown, the $N = 2$ state also exceeds the P_{YZ} gap, a similar $2 \rightarrow 1$ I_q transition soon follows. The system is now in $|1\rangle$ again, and the process repeats. This Josephson-plus-quasiparticle (JQP) cyclic process does give current, by repeated tunneling of single electrons through J_{YZ} and of pairs through J_{XY} . After many repeats the cycle will be interrupted by a $1 \rightarrow 0$ transition. The system

then hops slowly among lower N levels until it happens to reenter the $N=1$ level and the JQP cycle starts anew. The essence of the effect is the I_q tunneling in one junction being fed by and feeding the level-mixing process in the other junction in cyclic fashion.

This picture accounts for several features of the data: (1) The position and in part the shape of the peak come about because the JQP cycle is efficient only for the window $2\Delta + e/2C' < V_X < 2\Delta + 3e/2C'$. For lesser V_X , $N=2$ is below the gap in P_{YZ} so the low $2 \rightarrow 1$ rate is a bottleneck. For greater V_X , $N=1$ moves above the gap and the $1 \rightarrow 0$ rate becomes large compared to that of $0 \rightarrow 1$, reducing the time spent in the cycle. (2) For fixed V_X the alignment occurs periodically with V_M as successive levels pass through the $V_X - V_Y = 0 \pm E_J$ region of strong mixing. This causes the periodic rise and fall of the peak with V_M , and also affects the peak shape by level movement with V_X . (3) The V_X and V_M at which peaks occur (these lie at the peak bases in Fig. 2) should fall on a line of $V_X - V_Y = 0$. From the capacitances and the pattern symmetry this line is bounded by the dotted lines in Fig. 2. (4) The peak size depends on the JQP cycle rate, some fraction of $I_c(XY)/2e$, reduced by the dead time spent in other levels. We have made simulations using BCS P_{ij} and assuming for the JQP cycle that mixing occurs via coherent oscillations, and that $N \rightarrow N \pm 1$ transitions occur at the P_{ij} given rates weighted by the probability that the system is in $|N\rangle$. The resulting $I(V_X, V_M)$ in Fig. 4(b) show a peak similar to that in the data, but ~ 3 times larger. This discrepancy may be because the dead time ($\sim 30\%$) is sensitive to small changes in P_{XY} and P_{YZ} below the gap. Alternately, the model may be insufficient, e.g., the lifetime of the $1 \rightleftharpoons 3$ oscillation is only $\sim \frac{1}{4}$ cycle at the peak, suggesting that a fuller quantum treatment may be needed. (5) One would expect a similar peak when levels align with $V_Y = 0$, with the roles of J_{YZ} and J_{XY} reversed. This peak would be small, however, because the $\sim 2.5:1$ ratio of resistances of J_{YZ} and J_{XY} means the system seldom visits levels near $V_Y = 0$ in the V_X window of (1). Simulations bear this out. For the more symmetric connection of S to V_X and $P+T$ to ground, two peaks do occur.

We must defer discussion of relevant issues such as temperature dependence (the peak persists to $T \sim 1$ K),

alternate wiring, behavior at low $V_X = 0$, effect of high B , and of other samples. In summation, we have observed Josephson effects in a limiting case of an effective two-level system. It is remarkable that even for $E_c \sim 5E_J$ and $kT \sim 10E_J$ the Josephson current is still able to carry a significant fraction of I_c .

We gratefully acknowledge extensive and very helpful computational assistance from R. C. Fulton.

¹I. Giaever and H. R. Zeller, Phys. Rev. Lett. **20**, 1504 (1968); H. R. Zeller and I. Giaever, Phys. Rev. **181**, 789 (1969).

²T. A. Fulton and G. J. Dolan, Phys. Rev. Lett. **59**, 109 (1987).

³L. S. Kuzmin and K. K. Likharev, Pis'ma Zh. Eksp. Teor. Fiz. **45**, 389 (1987) [JETP Lett. **45**, 495 (1987)].

⁴J. S. Barner and S. T. Ruggiero, Phys. Rev. Lett. **59**, 807 (1987).

⁵P. J. M. Van Bentum, R. T. M. Smokers, and H. Van Kempen, Phys. Rev. Lett. **60**, 2543 (1969).

⁶J. Lambe and R. C. Jaklevic, Phys. Rev. Lett. **22**, 1371 (1969).

⁷R. H. Ono, M. J. Cromar, R. L. Kautz, R. J. Soulen, J. H. Colwell, and W. E. Fogle, IEEE Trans. Magn. **23**, 1670 (1987).

⁸M. Iansiti, A. T. Johnson, C. J. Lobb, and M. Tinkham, Phys. Rev. Lett. **59**, 489 (1987); M. Iansiti, M. Tinkham, A. T. Johnson, W. E. Smith, and C. J. Lobb, Phys. Rev. B **39**, 6465 (1989).

⁹A. Widom, G. Magaloudis, T. D. Clark, H. Prance, and R. J. Prance, J. Phys. A **15**, 3877 (1982).

¹⁰K. K. Likharev, *Dynamics of Josephson Junctions and Circuits* (Gordon and Breach, New York, 1986).

¹¹E. Ben-Jacob and Y. Gefen, Phys. Lett. **108A**, 298 (1985).

¹²K. K. Likharev and A. B. Zorin, J. Low Temp. Phys. **59**, 347 (1985).

¹³F. Guinea and G. Schön, J. Low Temp. Phys. **69**, 219 (1987).

¹⁴M. Büttiker, Phys. Rev. B **35**, 4737 (1987).

¹⁵K. K. Likharev, IBM J. Res. Dev. **42**, 144 (1988).

¹⁶K. Mullen, Y. Gefen, and E. Ben-Jacob, Physica (Amsterdam) **152B**, 172 (1988); K. Mullen, E. Ben-Jacob, R. C. Jaklevic, and Z. Schuss, Phys. Rev. B **37**, 98 (1988).

¹⁷K. K. Likharev, IEEE Trans. Magn. **23**, 1142 (1987).

¹⁸R. A. Ferrell and R. E. Prange, Phys. Rev. Lett. **10**, 479 (1963).